

DOI: 10.1002/adfm.200600587

# Inkjet Printing of Luminescent CdTe Nanocrystal–Polymer Composites\*\*

By Emine Tekin, Patrick J. Smith, Stephanie Hoepfener, Antje M. J. van den Berg, Andrei S. Susha, Andrey L. Rogach,\* Jochen Feldmann, and Ulrich S. Schubert\*

Dedicated to Prof. Dr. Piet J. Lemstra on the occasion of his 60th birthday

Inkjet printing is used to produce well-defined patterns of dots (with diameters of ca. 120  $\mu\text{m}$ ) that are composed of luminescent CdTe nanocrystals (NCs) embedded within a poly(vinylalcohol) (PVA) matrix. Addition of ethylene glycol (1–2 vol %) to the aqueous solution of CdTe NCs suppresses the well-known ring-formation effect in inkjet printing leading to exceptionally uniform dots. Atomic force microscopy characterization reveals that in the CdTe NC films the particle–particle interaction could be prevented using inert PVA as a matrix. Combinatorial libraries of CdTe NC–PVA composites with variable NC sizes and polymer/NC ratios are prepared using inkjet printing. These libraries are subsequently characterized using a UV/fluorescence plate reader to determine their luminescent properties. Energy transfer from green-light-emitting to red-light-emitting CdTe NCs in the composite containing green- (2.6 nm diameter) and red-emitting (3.5 nm diameter) NCs are demonstrated.

## 1. Introduction

Inkjet printing is an attractive technology for microscale patterning since it can eject tiny droplets (with diameters in the range 50–100  $\mu\text{m}$ ), which are composed of either solutions or dispersions of functional materials, onto addressable sites on a substrate. The main advantage of this technique is that it uses an additive approach, thus allowing significant cost savings as a consequence of the very low generation of waste. Further advantages are the ease of use and an increased choice of substrate upon which to print. Inkjet printing is a popular choice for use in the fabrication of devices such as light-emitting devices (LEDs), solar cells, and field-effect transistors.<sup>[1–6]</sup> Another major advantage of this technique is the ability of multiple depositions on one substrate, which is desired for printing

multicolor polymer LED's, and for combinatorial materials research.<sup>[7,8]</sup>

Semiconductor nanocrystals (NCs), have recently generated great interest with respect to their potential application in optoelectronics.<sup>[9–12]</sup> The most promising features of NCs are their high photochemical stability and their size-dependent optical properties, which result from the quantum-confinement effect. This means that the color of the photoluminescence (PL) of NCs can be tuned by varying their mean size.<sup>[13–15]</sup> Important issues for the envisaged optoelectronic applications of the NCs are the preservation of the relatively high PL efficiency in the NC-containing films and uniform distribution of NCs within the films together with their uniform optical quality. To satisfy these requirements, a suitable polymer that does not quench the luminescence intensity of NCs must be chosen as a matrix material, which also has to provide a homogeneous NC distribution.

One of the problems that needs to be addressed for inkjet printing of functional materials is that the as-printed patterns often display a morphological phenomenon commonly called “coffee staining”. This describes the accumulation of significant quantities of material at the edges of a printed structure, that is, features that are intended to be uniform dots take a pronounced cylindrical appearance instead. Deegan et al.<sup>[16]</sup> determined two conditions that were responsible for the ring formation. The first is that the contact line (i.e., the interface between ink, substrate, and air) has to be pinned, and the second is that evaporation has to occur from the edge of the deposited droplet. When the contact line is pinned, the evaporative loss of solvent from the edge must be replenished by a flow of liquid from the interior; this outward flow results in a preferential deposition of solute at the boundary. Obviously, if the features obtained for a printed solution containing NCs are

[\*] Dr. A. L. Rogach, Prof. U. S. Schubert, Dr. A. S. Susha, Prof. J. Feldmann  
Photonics and Optoelectronic Group  
Physics Department & Center for Nanoscience (CeNS)  
Ludwig-Maximilians-Universität München  
Amalienstr. 54, 80799 Munich (Germany)  
E-mail: andrey.rogach@physik.uni-muenchen.de;  
u.s.schubert@tue.nl

Prof. U. S. Schubert, E. Tekin, Dr. P. J. Smith, Dr. S. Hoepfener,  
A. M. J. van den Berg  
Laboratory of Macromolecular Chemistry and Nanoscience  
Eindhoven University of Technology (TU/e)  
P.O. Box 513, 5600 MB Eindhoven (The Netherlands)

Prof. U. S. Schubert, E. Tekin, Dr. P. J. Smith, A. M. J. van den Berg  
Dutch Polymer Institute (DPI)  
P.O. Box 902, 5600 AX Eindhoven (The Netherlands)

[\*\*] This work forms part of the DPI research program (project 448) and was further supported by NWO, the Leibniz program of the DFG and the Fonds der Chemischen Industrie.

not uniform then the resultant performance will be unsatisfactory with respect to optoelectronic applications. Suppressing this natural propensity of inkjet-printed material to form annular structures is a significant challenge. However, if one adopts a strategy that ensures that the above-mentioned conditions are not met then ring formation can be suppressed. One such approach involves printing from a two-solvent system, where one of the solvents has a higher boiling point than the other, which leads to a decreased rate of evaporation at the contact line.<sup>[17]</sup>

In this paper, we report inkjet printing of well-defined dots (with diameters of about 120  $\mu\text{m}$ ) of water-soluble luminescent CdTe NCs (stabilized with thioglycolic acid (TGA) or 3-mercaptopropionic acid (MPA)) embedded in a PVA matrix and subsequent studies of their morphology and PL. The homogeneity of dot thickness was sufficiently improved by the addition of 2 vol % of ethylene glycol, which prevented the “coffee stain” effect. After optimizing the morphology of the printed nanocomposites, we prepared combinatorial libraries of CdTe NC–PVA films in which the concentration of PVA in solution and the size of CdTe NCs were varied. The emission properties of these libraries were characterized in a parallel fashion using a UV/fluorescence plate reader. The results showed that the emission intensity of the CdTe NCs in the composite films with polymers can be improved by optimizing the NP/polymer ratio. Finally, the energy transfer between different size CdTe NCs within the same PVA matrix has been demonstrated.

## 2. Results and Discussion

The inkjet printer used for this study employed the drop-on-demand method, whereby droplet placement was achieved by mechanically positioning the substrate directly underneath the print head, which then generates the droplet. Droplet formation was achieved by changing the voltage across the piezoelectric ceramic that surrounds the ink chamber. This voltage change resulted in a pressure pulse, which in turn caused a column of ink to be ejected from the print-head’s orifice. This column rapidly assumed the familiar droplet shape, due to surface tension. Inks must be formulated to fit the physical and rheological requirements of fluid flow in the print head, with special consideration given to viscosity. If the ink is too viscous, then a large pressure pulse is needed to generate a droplet; whereas if the surface tension is too low, the print head generates satellites besides the desired droplet. These satellites reduce the resolution of the final deposit; therefore, new ink formulations are always optimized in order to obtain the parameters necessary for the production of single droplets. The two main parameters that were varied in this study were the voltage (that is applied across the piezoelectric actuator) and the pulse width (which is the time taken for the voltage to return back to its starting value).

Uniform, stable droplets of aqueous CdTe NCs solution were formed at 60–65 V and pulse widths of 30–35  $\mu\text{s}$ . Upon addition of polymers, the solutions became more viscous, and the values of voltage and pulse width subsequently increased. This re-

quired further optimization of the printing conditions for each NCs–polymer solution. Thus, solutions containing 1 wt % PVA (with a viscosity of 1.7 mPa s) were optimally ejected applying 85–90 V and 40  $\mu\text{s}$ . After the optimal voltages and pulse widths were determined, CdTe NC solutions containing 1 wt % PVA were printed both onto ITO-coated glass slides (ITO: indium tin oxide) and ozone-treated glass slides. These printed dots were analyzed using an optical profilometer in order to obtain information on their topographies. The dots of CdTe NCs–PVA composites exhibited ‘ring formation’,<sup>[18,19]</sup> that is, they had non-uniform structures whose edges were much higher than their centers (Fig. 1a). As discussed above, this ring structure results as a consequence of a higher evaporation rate at the droplet’s edge and a pinned contact line.<sup>[18]</sup> As we reported previously, the addition of a higher boiling point solvent to the ink improves the deposit’s homogeneity since evaporation at the contact line is reduced.<sup>[17,20]</sup> With this in mind, we tested ethylene glycol (boiling point 196–198 °C, water miscible) as an additive to the aqueous CdTe NCs–polymer solutions and investigated its influence on the patterns of the nanocomposites after drying was complete.

Solutions of CdTe NCs containing 1 wt % PVA, in which the amount of ethylene glycol varied from 0 to 20 vol %, were printed both onto ITO and glass. These substrates were placed onto a heated platform that was kept at 70 °C (as the increase in mass at the edge of a printed feature is time-dependent,<sup>[16]</sup> printing onto a heated substrate reduces the severity of “coffee staining” since the evaporation rate at all points on the deposited feature is increased). The dried patterns of the printed dots were characterized using an optical profilometer and found to be similar for both glass and ITO. Figure 1 shows the height profiles of the printed composites from different solvent compositions on glass. As can be seen from Figure 1a, the dot printed using 100 % water revealed a high side wall and a diameter of approximately 200  $\mu\text{m}$ . An addition of 2 vol % ethylene glycol (Fig. 1b) resulted in a uniform and homogeneous dot with a diameter reduced to 130  $\mu\text{m}$ . However, further additions of ethylene glycol, 5 vol % (Fig. 1c) and 10 vol % (Fig. 1d), caused the dot diameter to increase and had a detrimental influence on uniformity. Table 1 summarizes the contact angles formed by the solutions with varying ethylene glycol contents and diameters of the dots printed from these solutions. The increase in diameter corresponded to a decrease in the contact angle, which was measured for these solutions at

**Table 1.** Measured contact angles at room temperature and the diameters of the dots of CdTe NCs–PVA composites printed from solutions with a varied ratio of water and ethylene glycol ratio on glass and ITO.

Ratio of water/ ethylene glycol [vol %]	Measured contact angle on glass [°]	Dot diameter on glass [ $\mu\text{m}$ ]	Dot diameter on ITO [ $\mu\text{m}$ ]
100:0	22.2	200	190
98:2	44.5	130	120
95:5	30.3	140	130
90:10	24.6	160	150
85:15	20.8	180	170
80:20	19.7	200	190

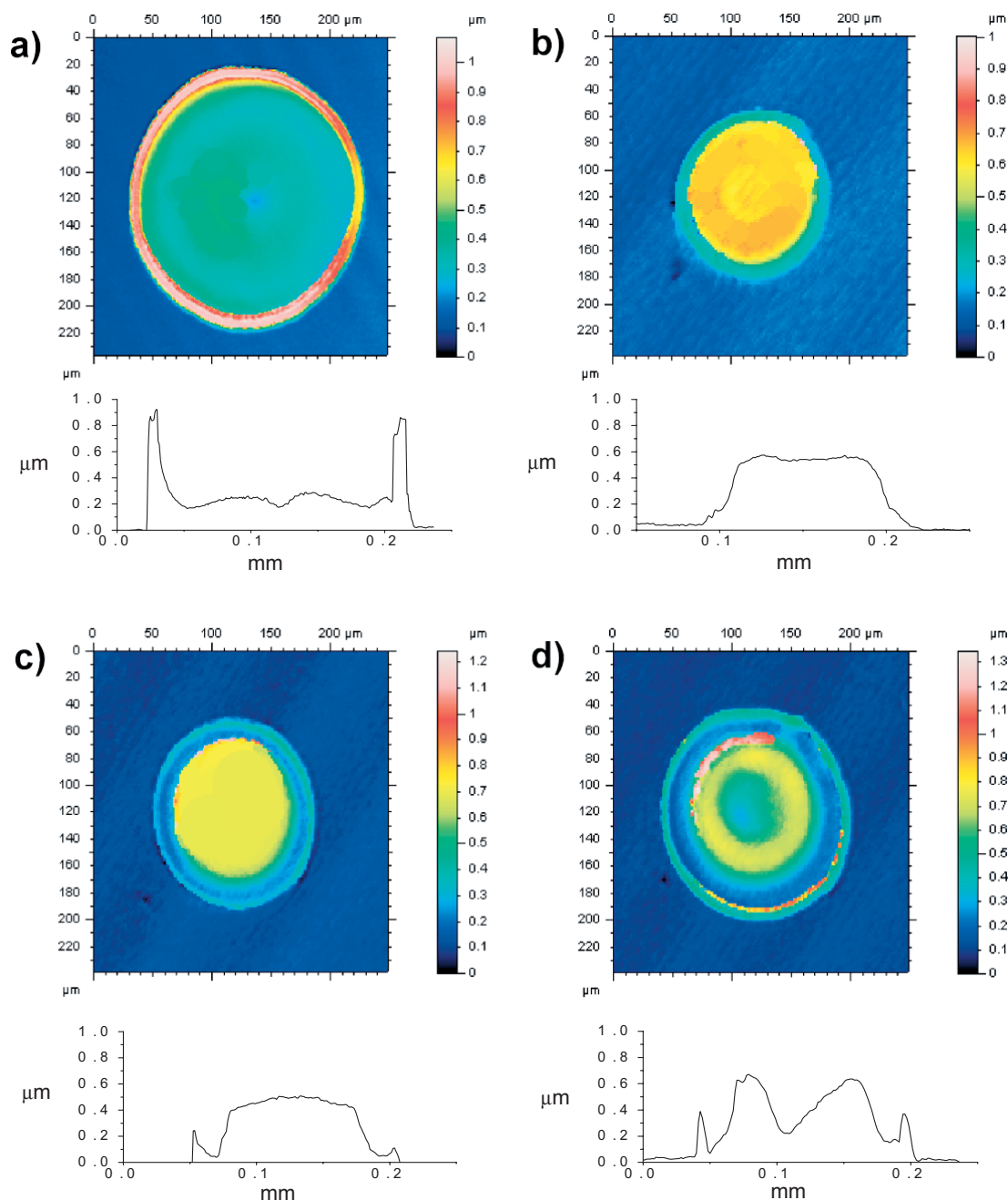


**Figure 1.** Optical profilometer images and cross sections of the composite films printed from CdTe NC solutions containing 1 wt% PVA in a) water, b) a water–ethylene glycol mixture (98:2 v/v), c) a water–ethylene glycol mixture (95:5 v/v), and d) a water–ethylene glycol mixture (90:10 v/v).

room temperature.<sup>[21]</sup> As can be seen from Table 1, with an increase of the ethylene glycol concentration, the contact angle decreased and the diameter increased. In addition, with increasing amounts of ethylene glycol the actual deposited droplet took longer to dry at all the points. Therefore, ring formation also occurred at higher glycol concentrations. As a consequence of these optimization studies, 2 vol% ethylene glycol in a solution of NCs and PVA was selected as the most suitable for inkjet printing of well-defined composite dots. A 3D image of a dot array of the CdTe NCs–PVA composite printed with this solvent ratio is shown in Figure 2.

Atomic force microscopy (AFM) studies on the surface topography of films printed on glass were performed for the samples printed both from a pure aqueous solution of CdTe NCs and from aqueous solutions of PVA/CdTe NCs (molar ratio is 15.6) blend. In the absence of polymer (Fig. 3a), the surface of the film was inhomogeneous revealing the presence of large aggregates (up to 100 nm in size). For the PVA-containing sample (Fig. 3b), the surface appeared to be much smoother, with some needle-like aggregates homogeneously distributed over the surface, alongside very tiny features which are attributed to the single polymer-embedded NCs. Thus, the PVA matrix pro-

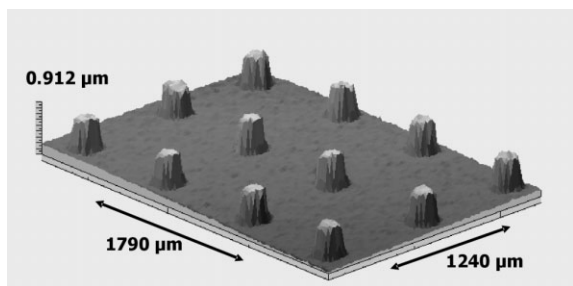


**Figure 2.** A 3D profilometer image of an array of dots printed from an aqueous PVA/CdTe NCs (molar ratio 15.6) solution containing 2 vol% ethylene glycol.

vides favorable conditions for the inkjet printing of homogeneous NC-containing layers. To investigate the effect of the polymer matrix on the luminescence properties of the embedded CdTe NCs, libraries of composite films containing PVA or poly(diallyldimethylammonium chloride) (PDDA) in different weight concentrations and CdTe NCs of different sizes and with different thiol stabilizer (TGA or MPA), were printed and characterized using fluorescence spectroscopy. The libraries were made up of 5 mm × 5 mm squares printed onto heated glass substrates (70 °C). Ethylene glycol was not added because the printed pixels had to fully wet the substrate in order to obtain large areas suitable for use within the UV/fluorescence plate reader. The dot spacing was 70 μm for these experi-

ments. Figure 4 shows the inkjet-printed library; reproducible and optically homogenous films were obtained.

When PDDA was used as a matrix, significant quenching of emission of the CdTe NCs was observed, which is attributed to the influence of the charges of this positively charged polyelectrolyte. In the case of the inert polymer (PVA), the emission of the embedded CdTe NCs remained strong in printed films, independently of the NC stabilizer. The library, which is shown in Figure 4, was created to study the influence of the polymer-to-NC ratio and NC size. The rows of this library varied in terms of NC size as described in Table 2. In each column, the

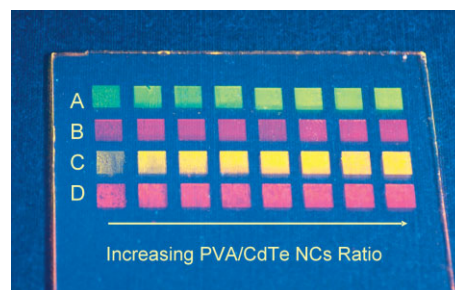


**Figure 4.** Photograph of an inkjet-printed combinatorial library of different size CdTe NCs emitting at different wavelengths (Table 2), including systematic variation of PVA content in the solution used for printing: from 0 to 1.4 wt% with an increment step of 0.2 wt%. Corresponding molar ratios of PVA/CdTe NCs in the films in each row are from 0 ( $0/1.6 \times 10^{-8}$ ) to 21.9 with an increment step of 3.12.

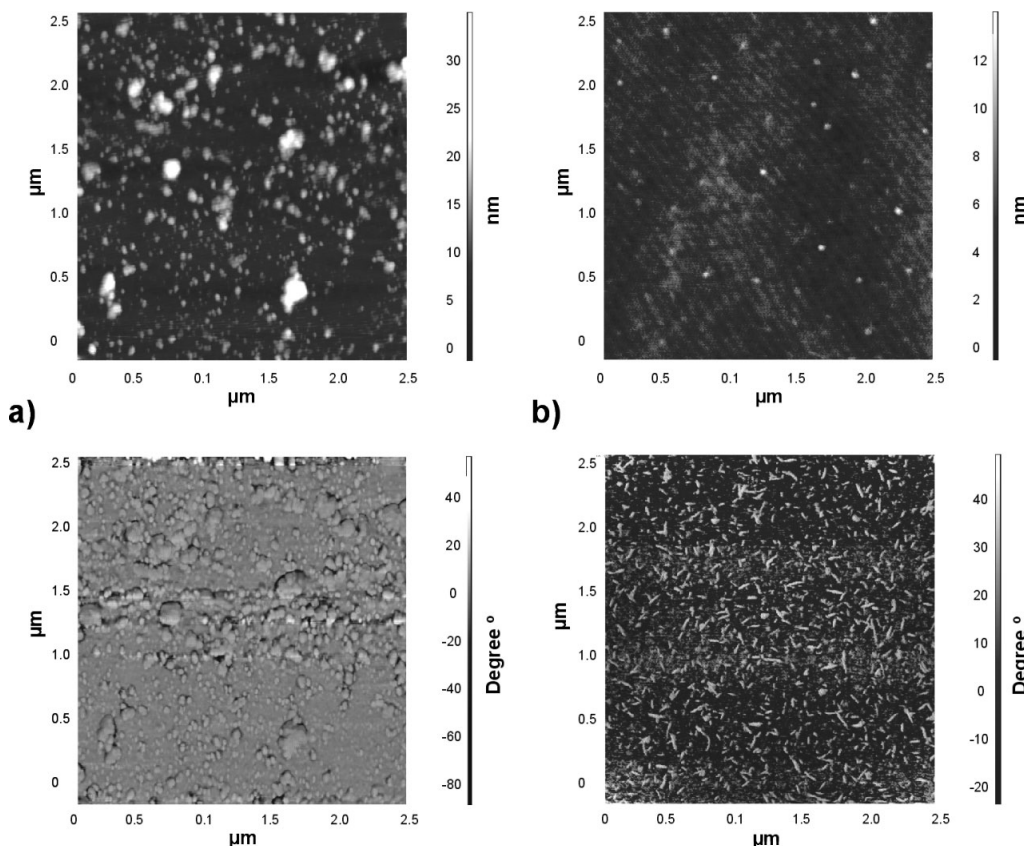


**Figure 3.** AFM height (top) and phase images (bottom) of the inkjet printed films of a) CdTe NCs and b) PVA/CdTe NCs (molar ratio 15.6) composites.

**Table 2.** Summary of particles sizes of the CdTe NCs used in the library shown in Figure 4, with corresponding PL colors and thiol stabilizer molecules, emission wavelengths of each row of the library, maximum increase in PL intensities caused by addition of polymer in comparison to the films of NCs without polymer, and the corresponding molar ratio of PVA/CdTe NCs responsible for the maximum achieved emission intensity.

Rows in the library	Particles size [nm]	Emission color	Stabilizer	Emission wavelength [nm]	Max increase in emission intensity [%]	Molar ratio of PVA/CdTe NCs with maximum intensity
A	2.6	green	MPA	565	70	12.50
B	3.5	red	TGA	640	73	15.62
C	3.0	yellow	MPA	590	270	15.62
D	3.8	red	MPA	675	1270	18.75

weight percent of PVA in solution used for printing varied in increments of 0.2 wt %, going from zero up to 1.4 wt % (corresponding molar ratios of PVA/CdTe NCs in the films in each row are from 0 ( $0/1.6 \times 10^{-8}$ ) to 21.9 with an increment step of 3.12). The emission spectra of each pixel, excited at 400 nm, are shown in Figure 5. In addition to the expected size-dependent variation of the emission of the CdTe NCs used, the emission intensity of each row systematically increased with increasing polymer amount until a maximum was reached. Table 2 summarizes the emission wavelengths of the printed pixels, maximum increase in emission intensities caused by addition of polymer in comparison to the films of NCs without polymer, and the corresponding molar ratio of PVA/CdTe NCs

responsible for the maximum achieved emission intensity. The increase in the PL intensity in the films where the NCs are surrounded by PVA can be explained as a consequence of an increase of the interparticle distance, which prevents the particle–particle interaction that causes self-quenching of the PL. This favorable effect saturates at some polymer concentration. At increasing polymer-to-NC ratios the absolute number of NCs in a film of given thickness

drops, leading to a decrease of the overall PL intensity. It causes PL-upon-polymer-amount dependence going through the maximum for all the rows in the library.

To further study the effects of particle–particle interactions in composite films, we printed another library which contained variable amounts of the small (2.6 nm), green-emitting CdTe NCs together with the large (3.5 nm), red-emitting CdTe NCs. The films were printed from water solutions of the mixtures of NCs containing 0.5 wt % PVA. Figure 6 shows a photograph of this library, together with the emission spectra obtained from the samples with different small-to-large NC ratios. The reduction of the PL intensity of the small (green-emitting) particles gradually took place, while emission of the larger particles (red-emitting) increased, pointing out the Förster resonant energy transfer (FRET) from the smaller donor NCs to the larger acceptor particles.<sup>[22]</sup> When the ratio of green emitters to red emitters was 85:15, the green emission peak disappeared completely, while the intensity of the red emission fed by the smaller particles continued to rise. Thus, efficient energy transfer between different size NCs in the printed composites results in more red emission from the films with a lower amount of red-emitting NCs, if they are fed by green-emitting counterparts.

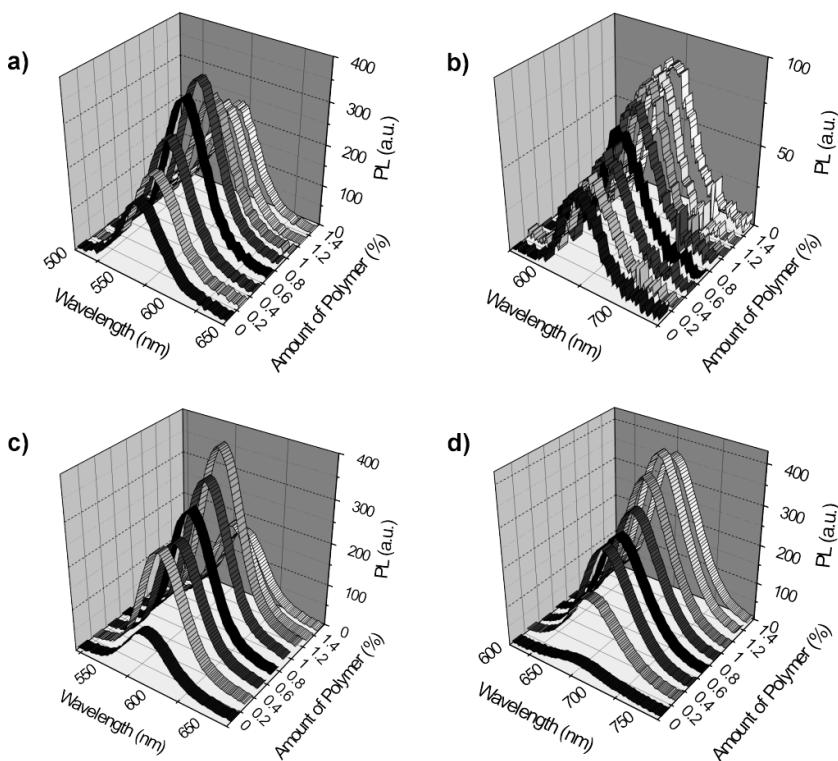


**Figure 5.** PL spectra taken from the libraries shown in Figure 4, a) the first row (green-emitting MPA-capped CdTe NCs–PVA), b) second row (red-emitting TGA-capped CdTe NCs–PVA), c) third row (yellow-emitting MPA-capped CdTe NCs–PVA), and d) the fourth row (red-emitting MPA-capped CdTe NCs–PVA).

### 3. Conclusions

We have demonstrated that high-quality homogeneous dots and arrays of dots composed of luminescent water-soluble CdTe NCs embedded in a PVA matrix can be fabricated by inkjet printing. The addition of ethylene glycol to the aqueous solution of CdTe NCs–PVA had a significant influence on the topography of the printed features; with 2 vol % being the most effective in suppressing the ring-formation effect. AFM characterization revealed that smoother films were formed when using PVA as a matrix compared to the NC-only layers. The emission of

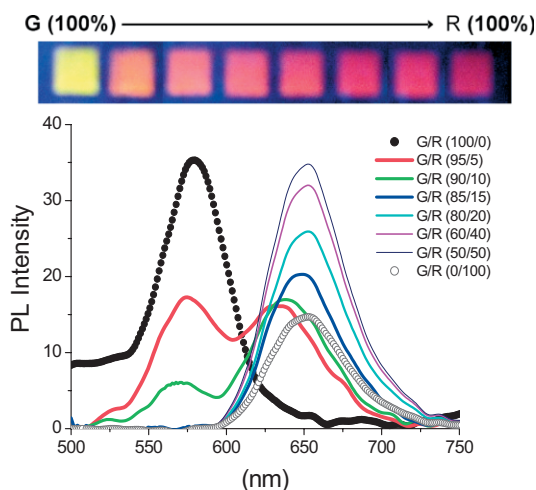


**Figure 6.** Photograph of an inkjet-printed library of the mixture of green- and red-emitting CdTe NCs (top). The PL spectra of this library (bottom).

CdTe NCs remained strong enough when they were embedded in PVA, while it was quenched by PDDA because of the influence of positive charges. The optimal PVA/CdTe NCs ratios in terms of the maximum available PL intensity was determined for different sizes of CdTe NCs by creation of combinatorial libraries measured in parallel by a UV/fluorescence plate reader. FRET was demonstrated in blends of the green- and red-emitting CdTe NCs within the same composite.

#### 4. Experimental

For the inkjet printing experiments, an Autodrop system (Microdrop Technology, Norderstedt, Germany) was used. This consists of an automated XYZ stage and a stroboscopic video camera, which is capable of printing solutions with viscosities of up to 20 mPa s. The diameter of the micropipette nozzle used was 70  $\mu\text{m}$ . The software of the system allows the programming of deposition patterns, such as matrixes or lines, and allows the user to define the number of droplets in the  $X$  and  $Y$  directions, as well as the spacing between each droplet.

The topographies of the printed patterns were measured using an optical profilometer, (Fogale Zoomsurf, France), which allows a vertical resolution of 7 nm and a horizontal resolution of 150 nm. A UV/fluorescence plate reader (Flashscan 530, AnalytikJena, Jena, Germany) was utilized to measure the respective fluorescence spectra of the NCs and their blends with the polymers. All of the films that were prepared for the combinatorial libraries could be conveniently excited at the same wavelength, namely 400 nm, regardless of the size of the NCs that they contained. AFM (Solver LS, NT-MDT, Russia) was used to investigate film morphologies utilizing Si cantilevers (NSG 11, NT-MDT, Russia).

The CdTe NCs used in this study were synthesized in water, employing either TGA or MPA as a stabilizer [23]. NCs of four different particle

sizes (2.6, 3.5, 3.0, and 3.8 nm) were used. The particle sizes were estimated from their extinction spectra following a literature procedure [24]. The concentration of CdTe NCs was ca  $10^{19}$  particles per liter in water. PVA (weight-average molecular weight  $M_w$ : 31 000–50 000  $\text{g mol}^{-1}$ , 99 % hydrolyzed), PDDA ( $M_w$ : 100 000–200 000  $\text{g mol}^{-1}$ ), and ethylene glycol were purchased from Aldrich. Microscope slides ( $3 \times 1$  inch) from Marienfeld (Lauda-Königshofen, Germany) and ITO coated glass slides from Präzisions Glass & Optik GmbH (Iserlohn, Germany) were used as substrates.

The substrates were ultrasonicated for 5 min in acetone. They were then cleaned with sodium dodecyl solution and washed with demineralized water to remove the soap. After ultrasonication in isopropanol for 5 min and drying with a  $\text{N}_2$  flow the slides were treated in a UV-ozone photoreactor (UVP PR-100, Upland, CA) for 20 min.

Received: July 2, 2006

Revised: August 22, 2006

Published online: November 16, 2006

- [1] J. Bharathan, Y. Yang, *Appl. Phys. Lett.* **1998**, *72*, 2660.
- [2] T. R. Hebner, C. C. Wu, D. Marcy, M. H. Lu, J. C. Sturm, *Appl. Phys. Lett.* **1998**, *72*, 519.
- [3] B. S.-C. Chang, J. Liu, J. Bharathan, Y. Yang, J. Onohara, J. Kido, *Adv. Mater.* **1999**, *11*, 734.
- [4] K. Cheng, M.-H. Yang, W. W. W. Chiu, C.-Y. Huang, J. Chang, T.-F. Ying, Y. Yang, *Macromol. Rapid Commun.* **2005**, *26*, 247.
- [5] R. F. Service, *Science* **2004**, *304*, 675.
- [6] B.-J. de Gans, P. C. Duineveld, U. S. Schubert, *Adv. Mater.* **2004**, *16*, 204.
- [7] Y. Yoshioka, P. D. Calvert, G. E. Jabbour, *Macromol. Rapid Commun.* **2005**, *26*, 238.
- [8] J. Wang, M. M. Mohebi, J. R. G. Evans, *Macromol. Rapid Commun.* **2005**, *26*, 304.
- [9] V. L. Colvin, M. C. Schlamp, A. P. Alivisatos, *Nature* **1994**, *370*, 354.
- [10] S. V. Kershaw, M. T. Harrison, A. L. Rogach, A. Kornowski, *IEEE J. Sel. Top. Quantum Electron.* **2000**, *6*, 534.
- [11] M. Gao, J. Sun, E. Dulkeith, N. Gaponenko, U. Lemmer, J. Feldmann, *Langmuir* **2002**, *18*, 4098.
- [12] S. Coe, W. K. Woo, M. Bawendi, V. Bulovic, *Nature* **2002**, *420*, 800.
- [13] L. Brus, *J. Phys. Chem.* **1986**, *90*, 2555.
- [14] A. P. Alivisatos, *Science* **1996**, *271*, 933.
- [15] A. L. Rogach, D. V. Talapin, H. Weller, in *Colloids and Colloid Assemblies* (Ed: F. Caruso), Wiley-VCH, Weinheim **2004**, p. 52.
- [16] R. D. Deegan, O. Bakajin, T. F. Dupont, G. Huber, S. R. Nagel, T. A. Witten, *Phys. Rev. E* **2000**, *62*, 756.
- [17] B.-J. de Gans, U. S. Schubert, *Langmuir* **2004**, *20*, 7789.
- [18] R. D. Deegan, O. Bakajin, T. F. Dupont, G. Huber, S. R. Nagel, T. A. Witten, *Nature* **1997**, *389*, 827.
- [19] R. D. Deegan, *Phys. Rev. E* **2000**, *61*, 475.
- [20] E. Tekin, B.-J. de Gans, U. S. Schubert, *J. Mater. Chem.* **2004**, *14*, 2627.
- [21] P. C. Duineveld, *J. Fluid Mech.* **2003**, *477*, 175.
- [22] T. Franzl, D. S. Koktysh, T. A. Klar, A. L. Rogach, J. Feldmann, *Appl. Phys. Lett.* **2004**, *84*, 2904.
- [23] N. Gaponik, D. V. Talapin, A. L. Rogach, K. Hoppe, E. V. Shevchenko, A. Kornowski, A. Eychmüller, H. Weller, *J. Phys. Chem. B* **2002**, *106*, 7177.
- [24] W. W. Yu, L. Qu, W. Guo, X. Peng, *Chem. Mater.* **2003**, *15*, 2854.